

Zero-energy resonance effects in atomic processes within a plasma environment

C F Clauser and R O Barrachina

Centro Atómico Bariloche and Instituto Balseiro, Comisión Nacional de Energía Atómica and Universidad Nacional de Cuyo, Av. Bustillo 9500, 8400 Bariloche, Argentina

E-mail: cesar.clauser@ib.edu.ar

Received 24 May 2016, revised 13 October 2016

Accepted for publication 24 October 2016

Published 18 November 2016



CrossMark

Abstract

We investigate the emergence of zero-energy resonance effects in atomic processes occurring within a plasma. By applying the final-state interaction theory we uncover the presence of these effects for particular configurations of density and temperature. We study the distortions that these resonances might produce in the corresponding cross sections whenever the relative momentum of a pair of charged particles intervening in the atomic process vanishes. We exemplify this general theory by applying it to the study of ionization processes by photon or ion impact. Finally we demonstrate that while for certain configurations of density and temperature these resonances might be blurred out by inhomogeneities; in others, the plasma might be tuned to the conditions for a zero-energy resonance, producing cross sections many times larger than standard estimates at the energy threshold.

Keywords: zero-energy resonance, atomic processes in plasmas, ionization, photoionization

(Some figures may appear in colour only in the online journal)

1. Introduction

The effect produced by the surrounding medium on the interaction of charged particles within a plasma leads to atomic spectra and cross sections that differ from those in vacuum. Since the seminal article by Debye and Hückel (1923), a large amount of experimental and theoretical research has been devoted to this effect, with consequences ranging from stellar physics to inertial confinement fusion. Various approaches, as for instance generalized variational methods (Stubbins 1993) and density functional theories (Gupta and Rajagopal 1982) have been employed to study atoms in dense plasmas (Rogers *et al* 1970, Dai *et al* 2001, Mukherjee *et al* 2002, Okutsu *et al* 2005), showing that the Debye screening might produce a strong distortion of the energy spectra of bound states. Furthermore, the effects produced by the plasma on scattering processes has also been profusely studied. For instance, inelastic collisions (including ionization of atoms and ions and charge transfer processes) by the impact of electrons (Hatton *et al* 1981, Deb and Sil 1984, Whitten *et al* 1984, Yoon and Jung 1996, Zhang *et al* 2010), positrons (Ghoshal *et al* 2013), photons (Jung 1998, Kar and Ho 2008, Lumb *et al* 2015), protons

(Scheibner *et al* 1987), He-like (Pandey *et al* 2013) and highly charged ions (Pandey *et al* 2012) have been analyzed in recent years. Of special interest for our study are the complex-coordinate rotation calculations performed by Ho and co-workers (see, for instance, Zhao and Ho 2004, Lin and Ho 2010, Sahoo and Ho 2010, Chang *et al* 2013) on the photoionization of atoms and ions near the ionization threshold.

These and other studies have demonstrated that not only the properties of bound states but also the scattering processes occurring within a plasma might be strongly influenced by its characteristics. Therefore, it is not possible to rely on atomic and scattering data measured or calculated in vacuum to represent what happens inside a plasma. This point becomes particularly crucial when these data are employed to analyze the performance and working conditions of fusion reactors.

Let us consider the transition matrix element \mathcal{T} for an arbitrary atomic process taking place within a plasma (Salzman 1998). Since the plasma can affect the interaction between the particles involved in the transition, it is very natural to presume that \mathcal{T} would not only depend on the parameters that characterize the corresponding scattering states, but also on those characterizing the plasma itself, as for

instance, its density and temperature. The purpose of this article is to discuss on very general grounds the kind of consequence that this dependence might have on an atomic transition occurring within a plasma, and whether it might lead to any sizeable effect.

In the following two sections we summarize the final-state interaction (FSI) theory and apply it to the study of an arbitrary atomic transition when the relative energy of two particles intervening in this process vanishes. In sections 4 and 5 we particularize these results to the case of Hulthén and Yukawa potentials, as working examples of the distortions produced on the corresponding cross section by a Debye screening effect, with special emphasis in section 6 on the appearance of zero-energy resonances. We illustrate these results, by applying them to ion-atom ionization and photoionization processes occurring within a plasma in sections 7 and 8, respectively. Finally, in section 9 we investigate the effects that inhomogeneities of the plasma might have on the results presented in the present article.

2. FSI theory

Let us analyze an atomic transition when the relative momentum k between a pair of particles vanishes. This two-body threshold might occur, for instance, in photoionization or radiative recombination processes, where the momentum k of the emitted (or absorbed) electron can be arbitrarily small depending on the relation between the energies of the absorbed (or emitted) photon and the initial (or final) bound state. Let us point out that in the present analysis, as it might be clear from the preceding example, k might be referring to the initial or final state of a two-body system, indistinctively.

According to the FSI theory (Gillespie 1964, Barrachina 1997, Fiol *et al* 2002), the $k \rightarrow 0$ limit of \mathcal{T} is dominated by the inverse of the s -wave Jost function $f_0(k)$ (Jost 1947, Jost and Pais 1951), namely

$$\mathcal{T} = \frac{1}{f_0(k)} \tilde{\mathcal{T}}, \quad (1)$$

where (Taylor 1972) (Atomic Units are used throughout this article, except where otherwise stated),

$$f_0(k) = 1 + \frac{2m}{k} \int_0^\infty e^{ikr} V_\lambda(r) \phi_{0k}(r) dr. \quad (2)$$

Here $V_\lambda(r)$ represents the potential between the two active particles of reduced mass m , relative momentum k and distance r ; and ϕ_{0k} is the regular solution of the corresponding s -wave radial Schrödinger equation, namely,

$$\left(\frac{d^2}{dr^2} + k^2 - 2mV_\lambda(r) \right) \phi_{0k} = 0, \quad (3)$$

which satisfies the condition,

$$\phi_{0k} \approx kr \quad \text{for} \quad r \rightarrow 0. \quad (4)$$

We have characterized the potential by means of a screening length λ as it is the case, for instance, in the Yukawa

potential,

$$V_\lambda^Y = -\frac{Z}{r} e^{-r/\lambda}. \quad (5)$$

The reduced transition matrix element $\tilde{\mathcal{T}}$ is usually approximated by \mathcal{T} itself, but evaluated without the interaction V_λ in the final state (see, e.g. Taylor 1972). However, this FSI ‘approximation’ might not always provide a realistic result. This is the case, for instance, in photoionization process (Clauser and Barrachina 2015a). Thus, it is customary to employ (1) as the actual definition of $\tilde{\mathcal{T}}$, representing a decomposition of the transition matrix element into one term, $\tilde{\mathcal{T}}$, which is mostly independent on the details of V_λ for $k \rightarrow 0$, and another one, $1/f_0(k)$, which might be strongly dependent on the FSI, and even lead to a zero-energy resonance for $k \rightarrow 0$. This factorization is not alien to that used for describing a Breit–Wigner resonance of energy E_R and width Γ , namely $\sigma_\ell(E) = \tilde{\sigma}_\ell(E)/(1 + \epsilon^2)$ with $\epsilon = 2(E - E_R)/\Gamma$; or as, for instance, in Fano (1961) and Shore (1967) parameterizations.

In our case, the decomposition (1) would allow us to describe in a general but very simple way how the screening effect produced by the plasma and characterized by the potential $V_\lambda(r)$ affects any particular atomic process where this interaction intervenes. In particular, the corresponding cross section would be distorted by a factor

$$F(k) = \frac{1}{|f_0(k)|^2}. \quad (6)$$

Finally, let us point out that even though in sections 7 and 8 we will be applying the present theory to the description of zero-energy resonances in ionization collisions and photoionization of hydrogenic atoms, the FSI formulation is not restricted to hydrogenic atoms or even to these particular atomic processes. Actually, it can and has been successfully applied to a variety of species and processes. Let us mention, for instance, the ionization of Ar atoms by the impact of neutral He (Barrachina 1990), the single-electron detachment of He^- (Báder *et al* 1997) and Li^- (Macri and Barrachina 2012) projectiles colliding with He and Ar gas targets or the photo-detachment of Li^- (see, e.g. Macri and Barrachina 2003, 2012 and references therein). Zero-energy resonances can also be observed in direct scattering processes, even if the intervening particles cannot form a bound state, as it will be explained in a following section.

3. S-wave Jost function

Let us summarize some general properties of $f_0(k)$ which are relevant to the present work. For instance, the phase of the Jost function is related to the s -wave phase shift of the standard non-relativistic scattering theory (Taylor 1972),

$$\delta_0(k) = -\arg f_0(k). \quad (7)$$

It can be also demonstrated that $f_0(k) \rightarrow 1$ for $k \rightarrow \infty$. On the other hand, under certain restrictive conditions on the potential $V_\lambda(r)$ thoughtfully explained by, for instance, Taylor

(1972), Newton (1982) and Burke and Joachain (1995), and which are generally verified by the Hulthén and Yukawa potentials considered in this article, the s -wave Jost function satisfies the following Taylor expansion in k (Macri and Barrachina 2013)

$$f_0(k) = [g_0 + g_2 k^2 + O(k^4)] + i[h_0 + h_2 k^2 + O(k^4)] k. \quad (8)$$

It can be demonstrated (Macri and Barrachina 2013) that the coefficients g_i and h_i (for $i = 0, 2, 4, \dots$) are real. Furthermore, in view of equation (7), the first four coefficients of this expansion, i.e. g_0, g_2, h_0 and h_2 , can be related to the scattering length a_0 and effective range r_0 of the well-known effective range expansion (Bethe 1949),

$$a_0 k \cot \delta_0(k) = -1 + \frac{1}{2} r_0 a_0 k^2 + O(k^4). \quad (9)$$

Actually, by replacing (8) and (9) in equation (7) and comparing the successive powers of k , we obtain (Macri and Barrachina 2013)

$$a_0 = \frac{h_0}{g_0}, \quad (10)$$

$$r_0 = \frac{2}{a_0} \left(\frac{h_2}{h_0} - \frac{g_2}{g_0} \right). \quad (11)$$

While the coefficients in the expansion (8) do not present singularities, i.e. they do not diverge as a function of λ (Macri and Barrachina 2013), the scattering length and the effective range might diverge for particular values of λ . This simple result would become of the outmost importance in the following sections for the description of the effects produced by a surrounding plasma on an atomic process. Even though it is not relevant to the present study, it might be worthwhile to mention that most of the previous discussion can be generalized to the case of ℓ -wave Jost functions, as thoughtfully explained by Macri and Barrachina (2013).

A very important characteristic of the Jost function is the relation between its zeroes and the bound states of $V_\lambda(r)$. In fact, it can be demonstrated (Taylor 1972) that each bound state of energy ϵ_0 of the potential $V_\lambda(r)$ is unequivocally related to a zero of the Jost function in the positive imaginary axis at $k = +i\sqrt{2m|\epsilon_0|}$. Now let us arbitrarily reduce the screening length λ . The zero will move towards the origin and eventually reach it. For reasons that will be explain later, this situation is referred to as a ‘zero-energy’ resonance. If we reduce λ even further, then this zero will continue along the negative imaginary axis. This zero, which no longer represents a bound state of $V_\lambda(r)$, is referred to as a ‘virtual’ state, in the understanding that it could become a bound state if the potential were more attractive.

Now, let us analyze the effect that these bound and virtual states, and in particular a zero-energy resonance, might produce on the distortion factor $F(k)$. We assume that the range of validity of the expansion (8) includes a region of

positive real (i.e. physical) values of k . Thus, we write

$$F(k) = \frac{1}{|f_0(k)|^2} \approx \frac{1}{g_0^2 + (h_0^2 + 2g_0g_2)k^2}. \quad (12)$$

We see that the distortion factor tends to a Lorentzian profile of height $1/g_0^2$ and width $\sqrt{a_0^2 + 2g_2/g_0}$. At a zero-energy resonance, i.e. whenever $f_0(0) = 0$, the coefficient g_0 vanishes and therefore, replacing in (12), we obtain that the distortion factor diverges like

$$F(k) \propto \frac{1}{h_0^2 k^2}, \quad (13)$$

for $k \rightarrow 0$. Let us finally point out that the previous Lorentzian shape is usually written as (see, e.g., Taylor 1972)

$$F(k) \propto \frac{a_0^2}{1 + a_0^2 k^2}. \quad (14)$$

But this expression is only valid near a zero-energy resonance (Macri and Barrachina 2002, 2013), i.e. for a bound or virtual state close to the origin, whenever the coefficient g_0 is small enough so that $g_0 \ll h_0^2/2g_2$.

4. Hulthén potential

As a working example of the general theory described in the previous section, let us consider the model potential proposed by Lamek Hulthén in 1942

$$V_\lambda^H(r) = -\frac{Z}{\lambda} \frac{e^{-r/\lambda}}{1 - e^{-r/\lambda}}. \quad (15)$$

It behaves as the Coulomb interaction at small distances and is exponentially screened for large values of r . In this respect, it resembles the Yukawa potential,

$$V_\lambda^Y = -\frac{Z}{r} e^{-r/\lambda}. \quad (16)$$

Far more important, the corresponding s -wave radial Schrödinger equation (3) can be solved analytically. The regular solution reads (Ford 1964)

$$\begin{aligned} \phi_{0k}^H(r) &= k\lambda e^{ikr}(1 - e^{-r/\lambda}) \\ &\times {}_2F_1(1 + i\kappa\lambda - ik\lambda, 1 - i\kappa\lambda - ik\lambda; 2; 1 - e^{-r/\lambda}), \end{aligned} \quad (17)$$

where ${}_2F_1$ is the hypergeometric function (Abramowitz and Stegun 1965) and

$$\kappa = k \sqrt{1 - \frac{2mZ\lambda}{(k\lambda)^2}}. \quad (18)$$

Now, replacing in (2), the integral can be analytically solved to get the following expression for the Jost function (Barrachina and Garibotti 1983),

$$f_0^H(k) = {}_2F_1(-i\kappa\lambda + ik\lambda, i\kappa\lambda + ik\lambda; 1, 1) \quad (19)$$

$$= \frac{\Gamma(1 - 2i\kappa\lambda)}{\Gamma(1 + i\kappa\lambda - ik\lambda) \Gamma(1 - i\kappa\lambda - ik\lambda)}. \quad (20)$$

Let us note that this Jost function depends only on two

dimensionless parameters, $k\lambda$ and $2mZ\lambda$. In particular,

$$g_0 = f_0(0) = \frac{1}{\Gamma(1 + \sqrt{2mZ\lambda}) \Gamma(1 - \sqrt{2mZ\lambda})} = \frac{\sin(\pi\sqrt{2mZ\lambda})}{\pi\sqrt{2mZ\lambda}} \quad (21)$$

becomes zero (i.e. produces a zero-energy resonance) whenever (Garibotti and Barrachina 1983),

$$2mZ\lambda = n^2 \quad \text{with } n = 1, 2, 3, \dots \quad (22)$$

As it was explained in the previous section, at these particular values of λ the s-wave bound energies,

$$\epsilon_{ns}^H = -\frac{mZ^2}{2n^2} \left(1 - \frac{n^2}{2mZ\lambda}\right)^2 \quad \text{with} \quad n = 1, 2, 3, \dots \leq \sqrt{2mZ\lambda}, \quad (23)$$

vanish.

By applying Euler's reflection formula for the Gamma function (Abramowitz and Stegun 1965)

$$\Gamma(1 - iz) \Gamma(1 + iz) = \frac{\pi z}{\sinh \pi z}, \quad (24)$$

we easily obtain the following expression for the distortion factor,

$$F^H(k) = \frac{1}{|f_0(k)|^2} = \frac{\pi mZ}{k} \frac{\sinh(2\pi k\lambda)}{\sinh^2(\pi k\lambda) - \sinh^2(\pi \kappa\lambda)}. \quad (25)$$

Note that, as expected, $F^H(k) \rightarrow 1$ for $k \rightarrow \infty$ or $Z \rightarrow 0$. On the other hand, for $k\lambda \ll \min\{1; \sqrt{2mZ\lambda}\}$, this enhancement factor takes a Lorentzian shape of height $1/g_0^2$ and width $|g_0\lambda|/\sqrt{2mZ\lambda}$, as explained in the previous section. Finally, at a zero-energy resonance,

$$F^H(k) \approx \left(\frac{2mZ}{nk}\right)^2 \quad \text{for } n = 1, 2, 3, \dots, \quad (26)$$

as it is shown in figure 3.

Let us now evaluate the enhancement factor $F(k)$ in the limit $\lambda \rightarrow \infty$, for which V_λ^H tends to the Coulomb potential $V^C(r) = -Z/r$ (Ma 1954). The limits $k \rightarrow 0$ and $\lambda \rightarrow \infty$ can not be taken independently (Kolsrud 1978), and therefore the Lorentzian shape is not valid anymore. Instead, we obtain,

$$F^C(k) = \frac{2\pi mZ/k}{1 - e^{-2\pi mZ/k}}, \quad (27)$$

which goes to unity for large values of k , as usual; but diverges like

$$F^C(k) \approx \frac{2\pi mZ}{k} \quad \text{for } k \rightarrow 0. \quad (28)$$

This behavior is radically different from the Lorentzian shape or even the $1/k^2$ divergence at zero-energy resonances, that are standard for screened potentials. This particular $1/k$ behavior can be ascribed to the presence of an accumulation point of the bound energy spectrum

$$\epsilon_n^C = -mZ^2/2n^2 \quad (29)$$

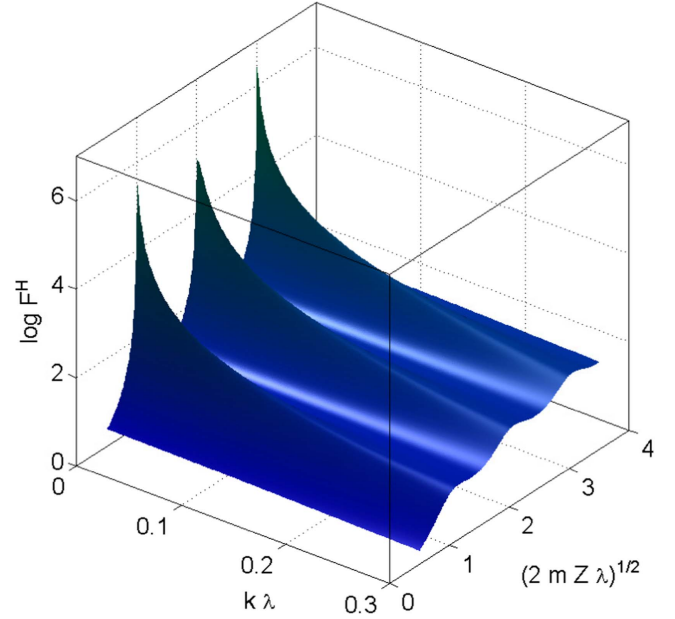


Figure 1. Enhancement factor F^H for the Hulthén potential, as given by equation (25), as a function of the dimensionless parameters $k\lambda$ and $\sqrt{2mZ\lambda}$. Note how a zero-energy occurs each time that $\sqrt{2mZ\lambda} = n$ with $n = 1, 2, 3, \dots$

at the ionization threshold.

Finally, let us point out that, as it was demonstrated by Wang (1992), since $V^C(r) \leq V_\lambda^H(r)$ for every r , then

$$\epsilon_n^C \leq \epsilon_{ns}^H \quad \text{for } n = 1, 2, 3, \dots \leq \sqrt{2mZ\lambda}, \quad (30)$$

as it can be readily verified.

5. Yukawa potential

Within a plasma, the effect of a charge Z can be represented (Ichimaru 1973, Krall and Trivelpiece 1973) by a Yukawa potential (Yukawa 1935)

$$V_\lambda^Y = -\frac{Z}{r} e^{-r/\lambda}. \quad (31)$$

To define the screening length, λ in terms of the plasma's temperature and density, let us first consider the well-known degeneracy parameter (Ichimaru 1987)

$$\theta = \frac{T}{E_F}, \quad (32)$$

which allows us to separate the quantum (or degenerate) region ($\theta \ll 1$) and the classical region ($\theta \gg 1$). Here $E_F = v_F^2/2$ is the Fermi energy, $v_F = (3\pi^2 N)^{1/3}$ is the Fermi velocity and N is the plasma number density. Then the screening length (Neufeld and Ritchie 1955, Arista and Brandt 1984, Clauser and Arista 2013) reaches the Thomas–Fermi limit

$$\lambda = \frac{v_F}{\sqrt{3} \omega_p} \quad (\theta \ll 1), \quad (33)$$

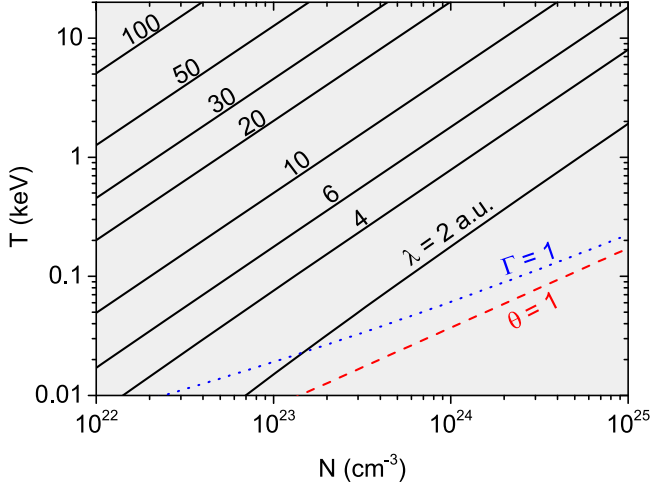


Figure 2. Debye screening lengths λ 's as function of density and temperature. The conditions $\theta = 1$ separate the classical and degenerate plasma regions, corresponding to the upper and lower parts of the figure, respectively. We also show the condition $\Gamma = 1$, which separates the correlated and uncorrelated regions, as explained in the text.

for low values of θ , while for $\theta \gg 1$ the Debye limit

$$\lambda = \sqrt{\frac{T}{4\pi N}} \quad (\theta \gg 1), \quad (34)$$

is obtained. Here $\omega_p = \sqrt{4\pi N}$ refers to the plasma frequency. As it was previously stated, all quantities are expressed in atomic units. Here we are assuming that the ion of charge Z is static with respect to the plasma, or moving with a velocity much smaller than $\lambda\omega_p$; an assumption that is consistent with the study of small relative electron-ion momenta k as considered in the present work.

Figure 2 shows different values of λ as function of density and temperature. We also show the conditions $\theta = 1$. Let us note that, at most of the values of T and N considered in the figure correspond to the classical region $\theta \gg 1$. In addition, we show the conditions $\Gamma = 1$, where

$$\Gamma = \frac{(4\pi N/3)^{1/3}}{E} \quad (35)$$

is the parameter that separate the correlated ($\Gamma \ll 1$) and uncorrelated ($\Gamma \gg 1$) regions. Here, E refers to the characteristic electron energy. For classical plasmas $E = T$ and, for degenerate plasmas, $E = E_F$ (Ichimaru 1982). In order to illustrate Γ in a continuous way, we use $E \approx T + E_F$ which is consistent with a quadratic electron velocity approximation.

As we have already demonstrated, all the results obtained in the previous sections are not unique to the Hulthén potential, but are generally valid for any screened Coulomb potential including, for instance, the cut-off Coulomb potential (Garibotti and Barrachina 1983),

$$V_\lambda^C(r) = -\frac{Z}{r} \Theta(\lambda - r), \quad (36)$$

whose s-wave Schrödinger equation can also be solved analytically (Garibotti and Barrachina 1983). Unfortunately, such an exact solution is not available for the Yukawa potential

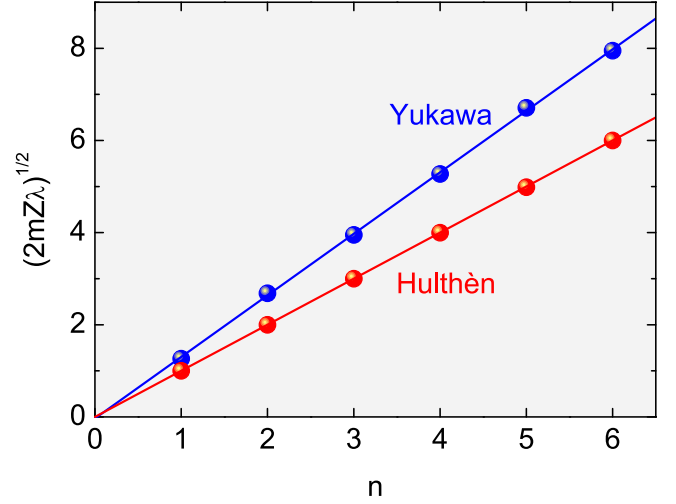


Figure 3. Critical values of $\sqrt{2mZ\lambda}$ for Yukawa and Hulthén potentials, at which a zero-energy resonance occurs, as a function of the quantum number n . The data corresponding to the Yukawa potential were extrapolated from the numerical calculation by Stubbins (1993).

(Hall 1992)

$$V_\lambda^Y = -\frac{Z}{r} e^{-r/\lambda}. \quad (37)$$

However, it is still valid that the energy spectrum of bound states verifies the same scaling rule than for the Hulthén potential,

$$\epsilon_{ns}^Y = mZ^2\epsilon_{ns}(\sqrt{2mZ\lambda}). \quad (38)$$

Furthermore, since $V_\lambda^H(r) \leq V_\lambda^Y(r)$ for $0 \leq r < \infty$, then (Wang 1992)

$$\epsilon_{ns}^H \leq \epsilon_{ns}^Y. \quad (39)$$

This means that for every particular value of the quantum number n , the corresponding zero-energy resonance has to occur for values of the dimensionless parameter $\sqrt{2mZ\lambda}$ that are larger for the Yukawa potential than for the Hulthén potential. This is corroborated in figure 3 which shows the values of $\sqrt{2mZ\lambda}$ at which a zero-energy resonance occurs as a function of the quantum number n for the Yukawa and Hulthén potentials. The data corresponding to the Yukawa potential were extrapolated from the numerical calculation by Stubbins (1993). The figure shows that $\sqrt{2mZ\lambda}$ also follows a simple linear dependency with n , as the one occurring for a Hulthén potential. A fitting of the data leads to

$$\sqrt{2mZ\lambda_Y} \approx \frac{4}{3} \sqrt{2mZ\lambda_H}, \quad (40)$$

for the critical values of $\sqrt{2mZ\lambda}$. Furthermore, a direct comparison with the numerical calculation by Stubbins (1993) shows that equation (23) provides a good approximation for the energies of s-wave bound states for the Yukawa potential whenever λ_H is re-scaled according to

equation (40), namely

$$\epsilon_{\text{ns}}^Y \approx -\frac{mZ^2}{2n^2} \left(1 - \frac{8n^2}{9mZ\lambda}\right)^2 \quad \text{with} \quad (41)$$

$$n = 1, 2, 3, \dots \leq \sqrt{9mZ\lambda/8}.$$

6. Zero-energy resonance

The $1/k$ divergence of the Coulomb enhancement factor (28) for $k \rightarrow 0$ is responsible for one of the most striking effect of Atomic Collisions Physics. In 1970 Crooks and Rudd observed a cusp-shaped peak in the energy spectrum of electrons emitted in the forward direction in the ionization of helium by the impact of energetic protons. This cusp occurred when the velocity of the electron matches that of the projectile, i.e., when the relative electron–proton momentum k vanishes. It was thoughtfully studied for decades, both theoretically and experimentally, being observed for a variety of ionic projectiles, including 90 MeV/u U^{+88} (Hillenbrand *et al* 2015), and even in positron-atom ionization collisions (Kövér and Laricchia 1998, Fiol *et al* 2001). By visualizing this effect in terms of a smooth continuation through the ionization limit of a capture of the electron by the proton into highly excited states of a hydrogenic atom, the name ‘electron capture to the continuum’ (ECC) was coined (Macek 1970). Being this so, the same existence of an ECC divergence was associated to the presence of an accumulation point of Rydberg states at the ionization threshold, i.e. to the Coulomb potential itself. The mere possibility of a similar effect being produced by a screened potential was simply ruled out. For instance, McGuire *et al* (1987) argued that, in view of the Uncertainty Principle, a screening of the Coulomb tail would lead to a truncated ECC cusp, with a width $\Delta k \approx \hbar/\lambda$. At that time it was already known (Garibotti and Barrachina 1983) that this argument was not entirely valid, since it was mistakenly relying on the screening length λ directly, instead of on the scattering length a_0 . As we have shown in the previous sections, the difference was not of minor importance, since it might lead to drastically different behaviors at the $k \rightarrow 0$ threshold. It can even produce a $1/k^2$ dependence in the case of a zero-energy resonance, resulting in a cusp even sharper than the one produced by the $1/k$ divergence corresponding to a pure Coulomb potential. Even so, the argument stated by McGuire *et al* (1987) was so convincing that it set the basis for assuming that the differential ionization cross section would not show any strong dependence on the electron-projectile momentum k for short-range potentials (see, e.g. Jakubaša-Amundsen 1989).

In 1989, the possibility of a ECC cusp occurring in the presence of a screened electron-projectile interaction was experimentally confirmed (Sarkadi *et al* 1989). In particular, a narrow ECC peak measured in coincidence with neutral He outgoing projectiles (Sarkadi *et al* 1989) was ascribed to the presence of a virtual state in the $e^- + \text{He}(2^1\text{S})$ system (Barrachina 1990, see also Macri and Barrachina 1998). This

hypothesis was initially received with disbelief (Jagutzki *et al* 1991, Salin 1994), but it was later confirmed by an experimental analysis of the dependence of the cusp on the fraction of metastable He states in the projectile’s beam (Kuzel *et al* 1993, Báder *et al* 1997, see also Schuch 1997).

Up to our knowledge, the first observation of a zero-energy resonance (Bethe 1949, Newton 1955) involved the singlet neutron–proton scattering, whose cross section at low impact energies is at least two orders of magnitude larger than geometrical estimated (see e.g. Eisenberg and Greiner 1976). Zero-energy resonances have also been actively investigated in relation with Bose–Einstein condensates. If the temperature is low enough, the elastic scattering of atoms can be described by the s-wave scattering a_0 alone (Huang 1987), and the presence of low-lying s-wave virtual or bound states might lead to extremely large values of a_0 , i.e. zero-energy resonances; as observed, for instance, in ^4He (Mester *et al* 1993), Cs (Arndt *et al* 1997) or triplet ^6Li collisions (Abraham *et al* 1997). The presence of zero-energy resonances have also been proposed in a variety of processes, ranging from the $p + p\mu$ scattering at very low energies (Kvitsinsky and Hu 1993) to atomic collisions in magnetic or optical ‘wave-guides’ (Bergeman *et al* 2003).

Our study is somewhat related to this last example of atomic processes occurring under confinement. Within a plasma the interaction between particles is screened by the surrounding media; with a Debye screening length λ that depends on the conditions of density N and temperature T . In view of the previous evidence, this means that for any atomic processes occurring in the interior of a plasma, the corresponding cross section might differ from that occurring in vacuum with pure Coulomb interactions, mainly whenever the relative energy of a pair of charged particles in the initial or final states vanishes.

In the following two sections we exemplify these conclusions by considering the effects produced by a Debye screening in ionization collisions and photoionization processes occurring within a plasma.

7. Ionization collisions

In view of the previous discussions, the cross section for an ionization collision within a plasma might be strongly distorted whenever the relative energy of the emitted electron with respect to the target or the projectile vanishes. Let us consider, for instance, the single ionization of an atom by the impact of an ion of charge Z .

$$P^{+Z} + T \rightarrow P^{+Z} + T^+ + e^-. \quad (42)$$

The double differential cross section (DDCS) for the emission of an electron of momentum \mathbf{k}_e reads (Fiol *et al* 2001)

$$\frac{d\sigma}{d\mathbf{k}_e} = (2\pi)^4 \frac{\mu K}{v} \int |\mathcal{T}|^2 d\hat{\mathbf{K}}. \quad (43)$$

Here, μ and \mathbf{K} are the reduced mass and relative momentum

of the $P^+Z + T^+$ system in the final state, respectively, and

$$\mathcal{T} = \langle \Psi_f | V | \Psi_i \rangle \quad (44)$$

is the transition matrix element where the state Ψ_i describes the initial target bound state and the projectile's free motion with velocity \mathbf{v} , while Ψ_f describes the stationary scattering state of the three-body system constituted by the electron (e), the projectile (P^+Z) and the residual target (T^+). Here, V is the interaction of P^+Z with both particles e^- and T^+ .

Let us first consider that the ionization process occurs 'in vacuum' (i.e. for $\lambda \rightarrow \infty$). Most perturbative models allow for the following FSI separation of the DDCS (see, e.g., Stolterfoht *et al* 1997 and references therein),

$$\frac{d\sigma}{d\mathbf{k}_e} = F^C(k_p) \times \frac{d\tilde{\sigma}}{d\mathbf{k}_e}, \quad (45)$$

where the distortion factor reads (see equation (27)),

$$F^C(k_p) = |e^{\pi Z/2k_p} \Gamma(1 - iZ/k_p)|^2 = \frac{2\pi Z/k_p}{1 - e^{-2\pi Z/k_p}}. \quad (46)$$

Here $\mathbf{k}_p = \mathbf{k}_e - \mathbf{v}$ is the relative momentum of the electron with respect to the projectile. This Coulomb distortion factor diverges like $1/k_p$ whenever k_p vanishes, i.e. at the electron–projectile ionization threshold, producing the well-known ECC cusp described in the previous section. The reduced DDCS $d\tilde{\sigma}/d\mathbf{k}_e$ does not diverge at $k_p = 0$, but reaches different limiting values along different directions \mathbf{k}_p (Shake-saft and Spruch 1978).

Let us now consider that the ionization process occurs within a plasma, so that the distortion factor $F^C(k)$ does no longer provide a valid description of the ECC cusp, and should be replaced by the distortion factor with the correct dependence on k_p and λ . Thus we replace it by the one corresponding to the Hulthén potential, according to equation (25),

$$F^H(k) = \frac{\pi Z}{k} \frac{\sinh(2\pi k \lambda_H)}{\sinh^2(\pi k \lambda_H) - \sinh^2(\pi \kappa \lambda_H)}, \quad (47)$$

but with the λ_H screening length corrected according to equation (40), namely $\lambda_H \approx 9\lambda/16$. Figure 4 shows this distortion factor for the single ionization of an atom within a plasma as a function of the electron momentum k_e in the forward direction (i.e. for \mathbf{k}_e parallel to \mathbf{v}). We clearly see a sizable distortion of the ECC cusp for different values of the screening length λ . Note that the enhancement factor verifies all the properties analyzed so far. For instance, it takes a Lorentzian shape for small values of k_p and, even though it is not evident in the figure, it goes to unity for $k_p \rightarrow \infty$. For $\lambda = 3.55$, the zero-energy resonance condition $\sqrt{9mZ\lambda/8} = 2$ is satisfied, and therefore a $1/k_p^2$ divergence occurs. On the other hand, the Gaussian shape is recovered for $\lambda = 2, 2.8$ and 7 , since $\sqrt{9mZ\lambda/8}$ gets the non-integer values $1.5, 1.775$ and 2.8 , respectively. In particular, since for $\lambda = 2$, $\sqrt{9mZ\lambda/8} \approx 1.5$ is halfway between the $\sqrt{9mZ\lambda/8} = 1$ and 2 resonances, the distortion produced by the enhancement factor is milder than in the other cases, as shown in the inset in figure 4. Finally, the usual $1/k_p$ divergence corresponding

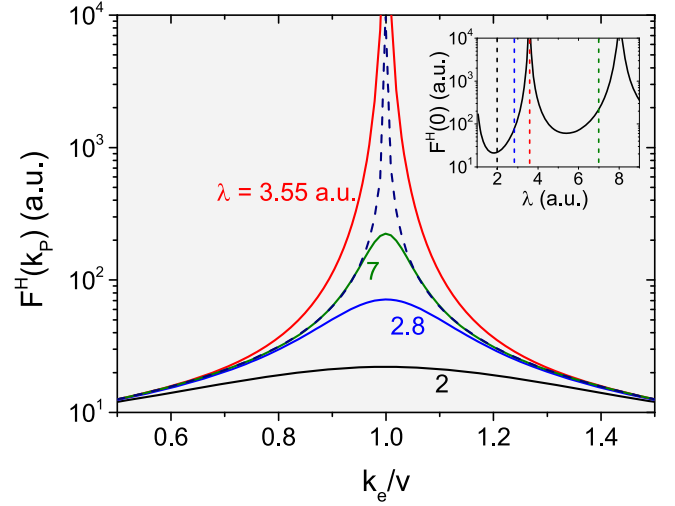


Figure 4. Electron capture to the continuum (ECC) peak for the single ionization of an atom by the impact of a proton of velocity $v = 1$ a.u. The enhancement factor is shown for the electron emitted in the forward direction (i.e. along the proton's velocity), as a function of the ratio of the electron and projectile velocities. The case corresponding to a pure Coulomb case (dashed line) is also shown for comparison. In the inset, the maximum of the enhancement factor is shown as a function of the screening length λ .

to a pure Coulomb case is also shown in the figure for comparison.

Here we have exemplified the kind of distortions that might occur in ionization collisions by considering the emission of a target electron by ion impact. However, it is important to point out that this effect does not depend on whether the electron is emitted from the target or from the projectile itself, in which case it is customarily known as an 'electron loss to the continuum' effect. The screening by the surrounding media in a plasma can similarly affect the so-called 'soft collision' peak, where the relative energy of the emitted electron with respect to the residual target vanishes (Stolterfoht *et al* 1997).

These results clearly show that the calculation of ionization collisions within a plasma should not be done with disregard to the corresponding screening effect, particularly when they are meant to be used in relation with the diagnosis of atom distributions in fusion reactors (Ning *et al* 2007).

8. Photoionization

In order to provide another example of the kind of effects that a zero-energy resonance might produce on an atomic process within a plasma, let us apply the previous results to a simple photoionization (PI) process,



where a single electron is emitted to the continuum with momentum \mathbf{k} by the absorption of a photon of wave vector \mathbf{k}_γ and polarization $\hat{e} (\perp \mathbf{k}_\gamma)$ by a Hydrogenic atom or ion A with

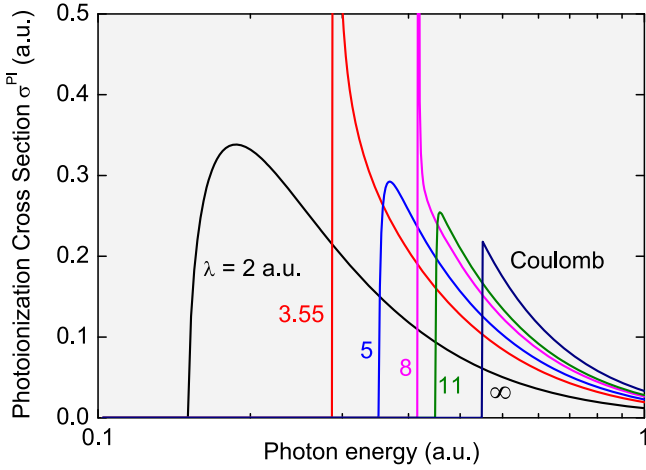


Figure 5. Total cross section σ^{PI} for the photoionization of a hydrogen atom within a plasma as a function of the photon energy for different values of the screening length λ .

ionization charge Z . The differential cross section reads

$$\frac{d\sigma^{\text{PI}}}{d\Omega_{\mathbf{k}}} = \frac{4\pi^2}{c^2} \frac{k}{k_{\gamma}} |\mathcal{T}|^2. \quad (49)$$

The non-relativistic transition matrix element \mathcal{T} reads

$$\mathcal{T} = \langle \psi_{\mathbf{k}} | e^{i\mathbf{k}_{\gamma} \cdot \mathbf{r}} \hat{\mathbf{e}} \cdot \nabla_{\mathbf{r}} | \phi \rangle, \quad (50)$$

where $\psi_{\mathbf{k}}$ is the final continuum state of the emitted electron and ϕ is the initial bound state. The same transition matrix element describes the radiative recombination process, where an atom captures an electron with emission of a photon. The corresponding differential cross section reads

$$\frac{d\sigma^{\text{RR}}}{d\Omega_{\mathbf{k}_{\gamma}}} = \frac{4\pi^2}{c^2} \frac{k_{\gamma}}{k} |\mathcal{T}|^2. \quad (51)$$

The total cross sections σ^{PI} and σ^{RR} are obtained by integrating over the solid angle and averaging on the polarization, verifying (for the ground state)

$$k_{\gamma}^2 \times \sigma^{\text{PI}} = k^2 \times \sigma^{\text{RR}}. \quad (52)$$

As we did in the previous section, let us first consider the photoionization ‘in vacuum’ (i.e. for $\lambda \rightarrow \infty$) of a Hydrogenic ground state

$$\phi(r) = \frac{Z^{3/2}}{\pi^{1/2}} e^{-Zr}, \quad (53)$$

of energy $-Z^2/2$ to a Coulomb continuum state

$$\begin{aligned} \psi_{\mathbf{k}}(\mathbf{r}) &= \frac{1}{(2\pi)^{3/2}} e^{i\pi Z/2k} \Gamma(1 - iZ/k) \\ &\times {}_1F_1(iZ/k, 1, i(kr + \mathbf{k} \cdot \mathbf{r})) e^{-i\mathbf{k} \cdot \mathbf{r}}. \end{aligned} \quad (54)$$

The transition matrix element \mathcal{T} can be analytically evaluated (Clauser and Barrachina 2015a) by means of Nordsieck’s method (Nordsieck 1954). The corresponding total cross section σ^{PI} is shown in figure 5 as a function of the photon energy

$$\epsilon = \frac{Z^2}{2} + \frac{k^2}{2} \quad (55)$$

for a hydrogen atom ($Z = 1$). In accordance to the FSI theory, as explained in section 2, the total photoionization cross section can be written as

$$\sigma^{\text{PI}} = F^C(k) \times \tilde{\sigma}^{\text{PI}}, \quad (56)$$

where $F^C(k)$ is the distortion factor for a pure Coulomb potential (see equations (27) and (46)), which diverges like $1/k$ for at the ionization threshold. However, note that since $\tilde{\sigma}^{\text{PI}} \propto k$ for small values of k , the photoionization cross section (56) does not diverges but reaches a finite value for $k \rightarrow 0$, as it can be seen in figure 5.

Now, when the photoionization process occurs within a plasma, $F^C(k)$ should be replaced by the distortion factor $F^H(k)$ for a screened electron–ion potential, as explained in previous sections. On the other hand, since the k dependence of $\tilde{\sigma}^{\text{PI}}$ does not vary significantly with λ , we will keep the calculation for a pure Coulomb potential, but with an effective ionization charge, as given by equation (41),

$$Z_{\text{eff}} \approx Z \left(1 - \frac{8}{9Z\lambda} \right), \quad (57)$$

affecting the initial bound state (53) and the corresponding energy, $-Z^2/2$, as well as the Coulomb continuum state (54) (but -of course- not the distortion factor F_H). Figure 5 shows the total cross section σ^{PI} for the photoionization of a hydrogen atom within a plasma as a function of the photon energy for different values of the screening length λ . We clearly see a sizable distortion of the cross section, even though this effect was mistakenly overestimated in a recent communication (Clauser and Barrachina 2015b).

We see that this simple model manages to reproduce the zero-energy resonances, which occur according to equation (22) at photon energies

$$\epsilon_n = \frac{Z^2}{2} \left(1 - \frac{1}{n^2} \right)^2 \quad \text{with } n = 1, 2, 3, \dots \quad (58)$$

Furthermore, the values of λ at which these zero-energy resonances occur,

$$\lambda = \frac{16}{18} \frac{n^2}{Z} \quad \text{with } n = 1, 2, 3, \dots, \quad (59)$$

are in reasonable agreement with those obtained in recent numerical complex-coordinate rotation calculations of photoionization of hydrogen and hydrogen-like helium (Zhao and Ho 2004, Lin and Ho 2010). For instance, the resonances observed in figures 1 and 2 in the article by Zhao and Ho (2004) and in figures 2 and 4 in the article by Lin and Ho (2010) match those for $n = 2$ obtained with our simple and general approach, as given by equation (58). Even the successive resonances evaluated by Lin and Ho (2010) for H and He^+ with a exponential-cosine-screened Coulomb potential verify the Z^{-1} and n^2 scaling rules predicted by equation (22). However, it is important to point out that in the article by Lin and Ho (2010), it was conjecture that they are shape-resonances resulting from quasi-bound np states. In our model, on the other hand, we propose that they are divergences occurring as a result of zero-energy resonance effects. In fact, the sharp form and strong asymmetry of the resonances evaluated

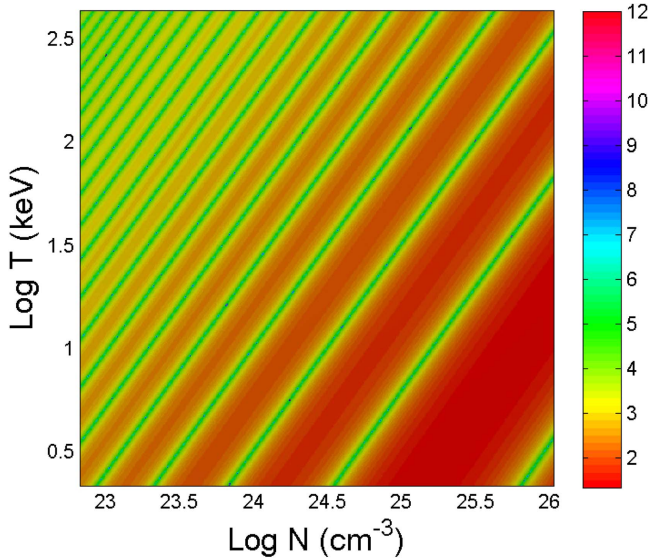


Figure 6. Distortion factor $F(k)$ evaluated at the $k = 0$ threshold as a function of the density N (cm^{-3}) and temperature T (keV) for an electron–proton interaction within a plasma.

by Zhao and Ho (2004) and Lin and Ho (2010) seem to be more consistent with zero-energy effects than with p shape-resonances.

9. Inhomogeneities

The screening length λ , being dependent of the density N and temperature T (see equation (34)), is not uniform all along the plasma. Therefore, the atomic transitions would occur under potentials with different values of λ , depending on the position within the plasma where they take place. The corresponding distortion factors $F(k)$ would also vary accordingly. Whenever this variation is small in comparison with the separation between resonant screening lengths, i.e. if the screening length is tuned to the zero-energy resonance, then this effect might produce a sizable effect. This is actually the case for values of λ of the order of some few atomic units, in the lower right section of figure 2, a condition that can be attained by a combination of low temperatures and/or high densities where, as shown in figure 6, the resonance conditions where $F(0)$ diverges, are well separated in N and T (Clauser and Barrachina 2015c). This means that zero-energy resonances might occur within the plasma and should be taken into account. On the other hand, the zero-energy resonances might be blurred by plasma inhomogeneities for combinations of density and temperature in the upper left section of figure 2. In this case, it would be necessary to replace the enhancement factor by an average over the range of variation of λ . In order to estimate this effect, let us assume that the screening length varies over a range of values including many zero-energy resonances with equal statistical weight. We integrate the distortion factor, equation (25), between two adjacent zero-energy resonances $\lambda_n = n^2/2mZ$

and $\lambda_{n+1} = (n + 1)^2/2mZ$,

$$\langle F^H(k) \rangle = \frac{1}{\lambda_{n+1} - \lambda_n} \int_{\lambda_n}^{\lambda_{n+1}} F^H(k) d\lambda \quad (60)$$

$$= \frac{\pi m Z}{k} \frac{1}{\lambda_{n+1} - \lambda_n} \times \int_{\lambda_n}^{\lambda_{n+1}} \frac{\sinh(2\pi k \lambda)}{\sinh^2(\pi k \lambda) - \sinh^2(\pi \sqrt{(k\lambda)^2 - 2mZ\lambda})} d\lambda. \quad (61)$$

As it is demonstrated in a previous article (Garibotti and Barrachina 1983), this average renders the distortion factor for a pure Coulomb potential,

$$\langle F^H(k) \rangle \approx F^C(k). \quad (62)$$

This means that when the screening length varies along a range of values larger than the separation between resonances, then the results corresponding to a non-screened potential are recovered as an average effect. Thus, for certain configurations of density and temperature, as it might be the case in magnetic confinement systems, it would seem as if the Debye screening were producing no effect, since the pure Coulomb case would be recovered as an average over the plasma's inhomogeneities.

10. Conclusions

In this article we have investigated the occurrence of zero-energy resonances in atomic processes within a plasma. We showed that this type of resonances might occur for particular conditions of density and temperature, whenever the relative energy of a pair of charged particles in the initial or final states vanishes. We applied this general and analytical description to the study of two particular atomic transitions, namely ionization collisions by ion impact and photoionization (and radiative recombination) processes. We demonstrated that the corresponding cross sections show zero-energy resonances at particular values of the Debye screening length.

It is important to point out that our theory is not limited to any of the particular examples considered in sections 7 and 8. They were chosen for pedagogical reasons and to simplify the calculation, which in the case studied in section 8 becomes completely analytical. We were also moved by the possibility of comparing our results with those by Lin and Ho (2010). In fact, as described in section 6, zero-energy resonances might occur in a variety of processes, including direct collisions; and by the action of virtual states, even in those cases where the intervening particles cannot form any bonding. This might be particularly relevant in the upper left corner of figure 2 (Ichimaru 1982), where the Saha equation of state at local equilibrium (Saha 1920) predicts an increasing proportion of ionized plasma.

Furthermore, even though we have centered our discussion on how an atomic process can be affected by a Debye screening, zero-energy resonances might appear in other atomic processes, and are not limited to a screened electron–

proton interaction or even to any particular choice of the potential between the intervening particles. For instance, the same theoretical description might be applied to the self-consistent average-atom model (see, e.g. Johnson *et al* 2006, Faussurier *et al* 2010, Starrett 2016) which, by including the plasma interactions in a more rigorous way, might be more valid than the Debye screening approximation for certain plasma conditions (Hu *et al* 2014).

Hence, even though for strongly coupled or quantum plasmas, the interaction between the acting particles may differ from the standard Yukawa potential (Shukla and Eliasson 2008), the appearance of zero-energy resonances is solely related to the presence of low lying bound or virtual states.

Independently of the description employed, the upper-left region of density and temperature in figures 2 and 6 correspond to an agglomeration of zero-energy resonances. Therefore the zero-energy resonances might be blurred by inhomogeneities in density and/or temperature; and the cross section for a pure non-screened potential should be recovered as an average effect. On the other hand, for particular combinations of density and temperature, the zero-energy resonance effects might produce sizable distortions of the cross sections, even order of magnitude larger than standard estimates. These results show that zero-energy resonances should not be ignored when studying atomic processes within a plasma, and their relevance in fusion devices should be taken into account.

Acknowledgments

This work was supported by the Comisión Nacional de Energía Atómica, CNEA (Controlled Nuclear Fusion Program) and Universidad Nacional de Cuyo (Grant 06/C416). CFC and ROB are also member of the Consejo Nacional de Investigaciones Científicas y Técnicas (CONICET), Argentina.

References

- Abraham E R I, McAlexander W I, Gerton J M, Hulet R G, Côté R and Dalgarno A 1997 *Phys. Rev. A* **55** R3299
- Abramowitz M and Stegun I A 1965 *Handbook of Mathematical Functions: With Formulas, Graphs, and Mathematical tables* (New York: Dover)
- Arndt M, Ben Dahan M, Guéry-Odelin D, Reynolds M W and Dalibard J 1997 *Phys. Rev. Lett.* **79** 625
- Arista N R and Brandt W 1984 *Phys. Rev. A* **29** 1471
- Báder A, Sarkadi L, Víkor L, Kuzel M, Závodszky P A, Jalowy T, Groeneveld K O, Macri P A and Barrachina R O 1997 *Phys. Rev. A* **55** R14
- Barrachina R O 1990 *J. Phys. B: At. Mol. Opt. Phys.* **23** 2321
- Barrachina R O 1997 *Nucl. Instrum. Methods B* **124** 198
- Barrachina R O and Garibotti C R 1983 *Lett. Nuov. Cim.* **36** 583
- Bergeman T, Moore M G and Olshanii M 2003 *Phys. Rev. Lett.* **91** 163201
- Bethe H A 1949 *Phys. Rev.* **76** 38
- Burke P G and Joachain C J 1995 *Theory of Electron-Atom Collisions, Part 1, Potential Scattering* (New York: Plenum)
- Chang T N, Fang T K and Ho Y K 2013 *Phys. Plasma* **20** 092110
- Clauser C F and Arista N R 2013 *Phys. Rev. E* **88** 053102
- Clauser C F and Barrachina R O 2015a *J. Phys. Conf. Ser.* **583** 012034
- Clauser C F and Barrachina R O 2015b *J. Phys. Conf. Ser.* **583** 012037
- Clauser C F and Barrachina R O 2015c *J. Phys. Conf. Ser.* **635** 052013
- Crooks G B and Rudd M E 1970 *Phys. Rev. Lett.* **25** 1599
- Dai S T, Solovyova A and Winkler P 2001 *Phys. Rev. E* **64** 016408
- Deb N C and Sil N C 1984 *J. Phys. B: At. Mol. Phys.* **17** 3587
- Debye P and Hückel E 1923 *Phys. Z.* **24** 185
- Eisenberg J M and Greiner W 1976 *Nuclear Theory* vol 3 (Amsterdam: North-Holland)
- Fano U 1961 *Phys. Rev.* **124** 1866
- Faussurier G, Blancard C, Cossé P and Renaudin P 2010 *Phys. Plasmas* **17** 052707
- Fiol J, Barrachina R O and Rodríguez V D 2002 *J. Phys. B: At. Mol. Opt. Phys.* **35** 149
- Fiol J, Rodríguez V D and Barrachina R O 2001 *J. Phys. B: At. Mol. Opt. Phys.* **34** 933
- Ford W F 1964 *Phys. Rev.* **133** B1616
- Garibotti C R and Barrachina R O 1983 *Phys. Rev. A* **28** 2792
- Gillespie J 1964 *Final State Interactions* (San Francisco: Holden-Day)
- Ghoshal A, Kamali M Z M and Ratnavelu K 2013 *Phys. Plasmas* **20** 013506
- Gupta U and Rajagopal A K 1982 *Phys. Rep.* **87** 260
- Hall R L 1992 *J. Phys. A: Math. Gen.* **25** 1373
- Hatton G J, Lane N F and Weisheit J C 1981 *J. Phys. B: At. Mol. Phys.* **14** 4879
- Hillenbrand P-M *et al* 2015 *Phys. Rev. A* **91** 022705
- Hu S X, Collins L A, Boehly T R, Kress J D, Goncharov V N and Skupsky S 2014 *Phys. Rev. E* **89** 043105
- Huang Cf K 1987 *Statistical Mechanics* (New York: Wiley)
- Hulthén L 1942 *Ark. Mat. Astr. Fysik A* **28** 1
- Ichimaru S 1973 *Basic Principles of Plasma Physics* (Reading: Benjamin)
- Ichimaru S 1982 *Rev. Mod. Phys.* **54** 1017
- Ichimaru S 1987 *Phys. Rep.* **149** 91
- Jagutzki O, Koch R, Skutlartz A, Kelbch C and Schmidt-Böcking H 1991 *J. Phys. B: At. Mol. Phys.* **24** 993
- Jakubassa-Amundsen D H 1989 *J. Phys. B: At. Mol. Opt. Phys.* **22** 3989
- Johnson W R, Guet C and Bertsch G F 2006 *J. Quant. Spectrosc. Radiat. Transfer* **99** 327
- Jost R 1947 *Helv. Phys. Acta* **20** 256
- Jost R and Pais A 1951 *Phys. Rev.* **82** 840–51
- Jung Y-D 1998 *Phys. Plasmas* **5** 4456
- Kar S and Ho Y K 2008 *Phys. Plasmas* **15** 013301
- Kolsrud M 1978 *J. Phys. A: Math. Gen.* **11** 1271
- Kövér Á and Laricchia G 1998 *Phys. Rev. Lett.* **80** 5309
- Krall N A and Trivelpiece A W 1973 *Principles of Plasma Physics* (New York: McGraw-Hill)
- Kuzel M, Sarkadi L, Pálkás J, Závodszky P A, Maier R, Berényi D and Groeneveld K O 1993 *Phys. Rev. A* **48** R1745
- Kvitsinsky A A and Hu C-Y 1993 *Phys. Rev. A* **47** 994
- Lin C Y and Ho Y K 2010 *Eur. Phys. J. D* **57** 21
- Lumb S and Nautiyal V 2015 *Eur. Phys. J. D* **69** 176
- Ma S T 1954 *Au. J. Phys.* **7** 365
- Macek J 1970 *Phys. Rev. A* **1** 235
- Macri P A and Barrachina R O 1998 *J. Phys. B: At. Mol. Opt. Phys.* **31** 1303
- Macri P A and Barrachina R O 2002 *Phys. Rev. A* **65** 062718
- Macri P A and Barrachina R O 2003 *Nucl. Instrum. Methods B* **205** 543
- Macri P A and Barrachina R O 2012 *J. Phys. Conf. Ser.* **397** 012005

- Macri P A and Barrachina R O 2013 *J. Phys. B: At. Mol. Opt. Phys.* **46** 06502
- McGuire J H, Reeves T, Deb N C and Sil N C 1987 *Nucl. Instrum. Methods B* **24/25** 243
- Mester J C, Meyer E S, Reynolds M W, Huber T E, Zhao Z, Freedman B, Kim J and Silvera I F 1993 *Phys. Rev. Lett.* **71** 71
- Mukherjee P K, Karwowski J and Dierksen G H F 2002 *Chem. Phys. Lett.* **363** 323
- Neufeld J and Ritchie R H 1955 *Phys. Rev.* **98** 1632
- Newton R G 1955 *Phys. Rev.* **100** 412
- Newton R G 1982 *Scattering Theory of Waves and Particles* (Berlin: Springer)
- Ning Y, Liu L, He B, Liu C L, Yan J and Wang J G 2007 *Phys. Rev. A* **75** 022713
- Nordsieck A 1954 *Phys. Rev.* **93** 785
- Okutsu H, Sako T, Yamanouchi K and Dierksen G H F 2005 *J. Phys. B: At. Mol. Opt. Phys.* **38** 917
- Pandey M K, Lin Y-C and Ho Y K 2012 *Phys. Plasmas* **19** 062104
- Pandey M K, Lin Y-C and Ho Y K 2013 *Phys. Plasmas* **20** 022104
- Rogers F J, Graboske H C Jr and Harwood D J 1970 *Phys. Rev. A* **1** 1577
- Saha M N 1920 *Phil. Mag.* **40** 472
- Sahoo S and Ho Y K 2010 *J. Quant. Spectrosc. Radiat. Transfer* **111** 52
- Salin A 1994 *Nucl. Instrum. Methods B* **86** 1
- Salzmann D 1998 *Atomic Physics in Hot Plasmas* (New York: Oxford University Press)
- Sarkadi L, Pálkás J, Kövér A, Berényi D and Vajnay T 1989 *Phys. Rev. Lett.* **62** 527
- Scheibner K, Weisheit J C and Lane N F 1987 *Phys. Rev. A* **35** 1252
- Schuch R 1997 *Nucl. Instrum. Methods B* **124** 443
- Shakeshaft R and Spruch L 1978 *Phys. Rev. Lett.* **41** 1037
- Shore B W 1967 *Rev. Mod. Phys.* **39** 439
- Shukla P and Eliasson B 2008 *Phys. Lett. A* **372** 2897
- Starrett C E 2016 *High Energy Density Phys.* **19** 58
- Stolterfoht N, DuBois R D and Rivaola R D 1997 *Electron Emission in Heavy Ion-Atom Collisions* (Berlin: Springer)
- Stubbins C 1993 *Phys. Rev. A* **48** 220
- Taylor J R 1972 *Scattering Theory: The Quantum Theory on Nonrelativistic Collisions* (New York: Wiley)
- Wang X R 1992 *Phys. Rev. A* **46** 7295
- Whitten L, Lane N F and Weisheit J C 1984 *Phys. Rev. A* **29** 945
- Yoon J-S and Jung Y-D 1996 *J. Phys. B: At. Mol. Opt. Phys.* **29** 3549
- Yukawa H 1935 *Proc. Phys. Math. Soc. Japan* **17** 48
- Zhang S B, Wang J G and Janev R K 2010 *Phys. Rev. A* **81** 032707
- Zhao L B and Ho Y K 2004 *Phys. Plasmas* **11** 1695